

Auditory evoked fields measured noninvasively with small-animal MEG reveal rapid repetition suppression in the guinea pig

G. Björn Christianson,¹ Maria Chait,¹ Alain de Cheveigné,² and Jennifer F. Linden^{1,3}

¹Ear Institute, University College London, London, United Kingdom; ²Laboratoire des Systèmes Perceptifs, Centre National de la Recherche Scientifique and École normale supérieure, Paris, France; and ³Department of Neuroscience, Physiology and Pharmacology, University College London, London, United Kingdom

Submitted 10 March 2014; accepted in final form 17 September 2014

Christianson GB, Chait M, de Cheveigné A, Linden JF. Auditory evoked fields measured noninvasively with small-animal MEG reveal rapid repetition suppression in the guinea pig. *J Neurophysiol* 112: 3053–3065, 2014. First published September 17, 2014; doi:10.1152/jn.00189.2014.—In animal models, single-neuron response properties such as stimulus-specific adaptation have been described as possible precursors to mismatch negativity, a human brain response to stimulus change. In the present study, we attempted to bridge the gap between human and animal studies by characterising responses to changes in the frequency of repeated tone series in the anaesthetised guinea pig using small-animal magnetoencephalography (MEG). We showed that 1) auditory evoked fields (AEFs) qualitatively similar to those observed in human MEG studies can be detected noninvasively in rodents using small-animal MEG; 2) guinea pig AEF amplitudes reduce rapidly with tone repetition, and this AEF reduction is largely complete by the second tone in a repeated series; and 3) differences between responses to the first (deviant) and later (standard) tones after a frequency transition resemble those previously observed in awake humans using a similar stimulus paradigm.

adaptation; magnetoencephalography; roving standard

MISMATCH NEGATIVITY (MMN) is one of the most investigated human brain responses. Classically, it is measured in the context of an “oddball” paradigm in which the brain response to rare deviant sounds is contrasted with that to a series of more common standards, revealing a negative shift in the evoked potential in the range of 100–250 ms after the sound onset. The mechanisms that produce MMN are the subject of some debate (May and Tiitinen 2010; Näätänen et al. 1978), but it is generally interpreted as reflecting the violation of predictions of a model tuned to an ongoing stimulus regularity (Lieder et al. 2013; Näätänen et al. 2007). Therefore, MMN has theoretical and practical appeal as a measure of brain activity that is hypothesized to tap sensory learning and adaptation to the statistics of the acoustic input. It has been put forward as a means of uncovering the mechanisms that enable listeners to adapt to complex listening environments (Garrido et al. 2013; Lieder et al. 2013), as a tool for probing perceptual representations, and as an assay for brain function in patients with neurological disorders (Boly et al. 2011; Näätänen et al. 2012).

Recently, the “roving standard” paradigm (Fig. 1B) has gained popularity as an alternative to the oddball paradigm method of eliciting MMN. The roving standard paradigm involves the use of sequences of repeated tone series with occasional step changes in frequency; tones immediately after

frequency transitions are deviant, and repeated tones are standards. Both tone frequencies are equally represented in the stimulus, thus controlling for physical differences between standard and deviant tones, and the experimental yield is higher than with the oddball paradigm (Cowan et al. 1993; Haenschel et al. 2005; Garrido et al. 2008). MMN increases in size with increasing number of preceding standards, and recent research has shown that this is mostly due to a reduction in the response to the repeated standards (“repetition suppression”) rather than an increase in the response to the deviants (e.g., Costa-Faidella et al. 2011; Haenschel et al. 2005). This finding carries important implications for understanding the mechanisms that give rise to the MMN response (Haenschel et al. 2005; Lieder et al. 2013).

In animal models, large brain-volume scale (synaptic potential-based) MMN studies using the classic oddball paradigm have yielded contradictory results (for a review, see Nelken and Ulanovsky 2007). Several investigations have failed to find an MMN-like response (Fishman and Steinschneider 2012; Lazar and Metherate 2003; Umbricht et al. 2005), resulting in a persistent mystery with respect to the neural generators of MMN. Such inconsistencies might stem from differing use of controls and the low yield associated with the oddball paradigm. At the single neuron level, stimulus-specific adaptation (SSA) (Ulanovsky et al. 2003), a phenomenon thought to be related to MMN or its precursors, has been demonstrated in various stages of the auditory system across a variety of species (Ayala and Malmierca 2012; Gutfreund 2012; Nelken and Ulanovsky 2007). However, the relationship between SSA and MMN remains unclear (Farley et al. 2010; Taaseh et al. 2011).

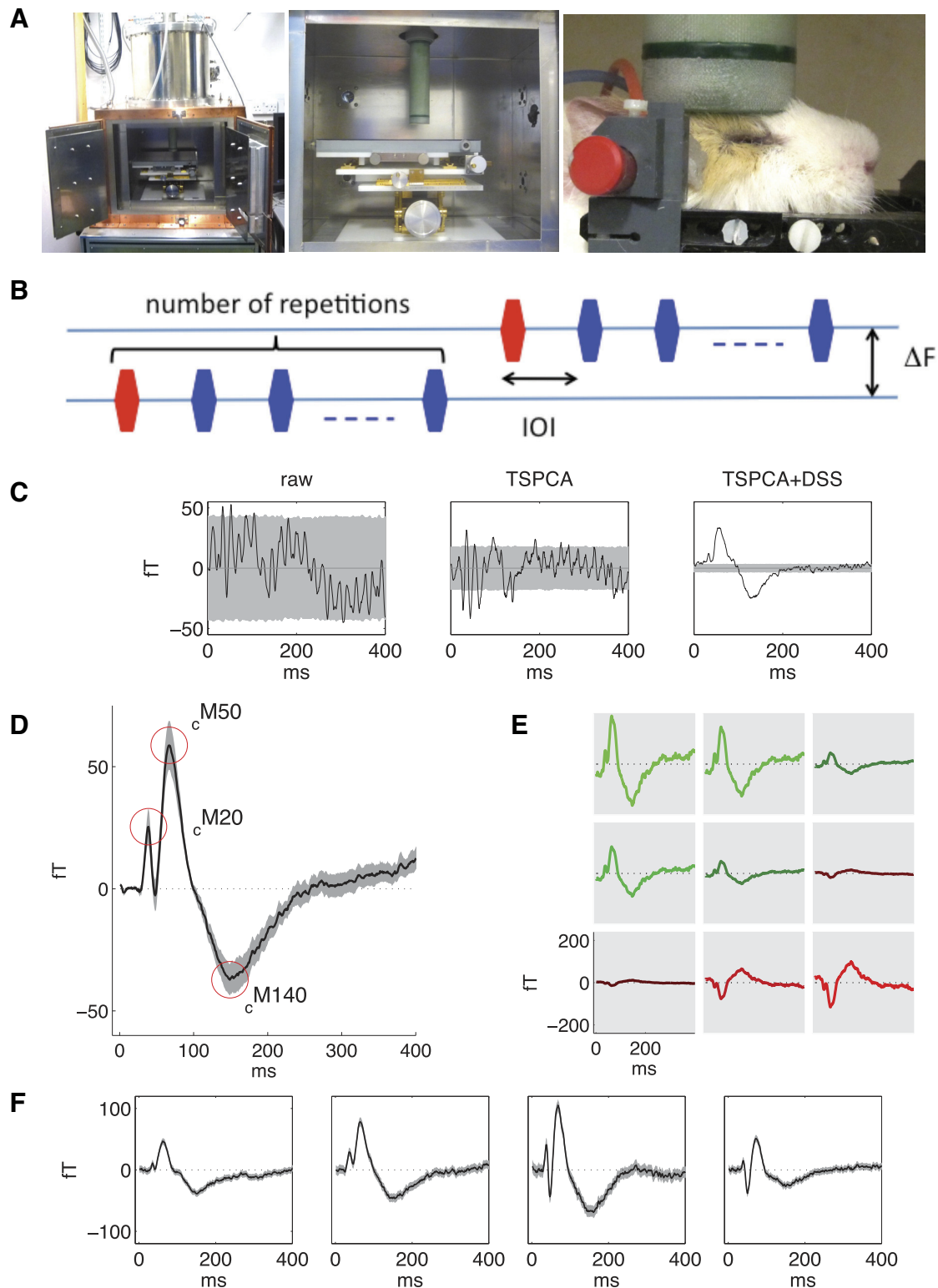
The present study constitutes part of an ongoing research effort to bridge the gap between human and animal investigations of MMN-like responses and SSA. We used the roving standard paradigm, adapted from recent work in humans (Costa-Faidella et al. 2011), to investigate auditory brain responses in the anaesthetised guinea pig, a rodent commonly used as an auditory model system because its low-frequency hearing range is similar to that of humans. We exploited a series of advances in instrumentation (Miyamoto et al. 2008) and signal processing (de Cheveigné and Parra 2014; de Cheveigné and Simon 2007) to provide the first characterization of auditory evoked fields (AEFs) obtained noninvasively using a multi-channel magnetoencephalography (MEG) system designed for recording from small animals, allowing comparison with similarly noninvasive MEG measurements of auditory brain responses in humans.

Address for reprint requests and other correspondence: J. F. Linden, Ear Institute, Univ. College London, 332 Gray's Inn Road, London WC1X 8EE, UK (e-mail: j.linden@ucl.ac.uk).

Our results validated the use of small-animal MEG to measure auditory brain responses in rodents and revealed an extremely rapid reduction in AEF amplitude with tone repetition. Moreover, we demonstrated that differences between deviant and standard responses in the roving standard paradigm analogous to reported MMN-like responses in awake human listeners can arise even in the anesthetised guinea pig.

METHODS

Small-animal MEG machine. Measurements were made using a purpose-built small-animal MEG machine designed and built by the Applied Electronics Laboratory of the Kanazawa Institute of Technology (Miyamoto et al. 2008) (Fig. 1A). The machine features a single sensor array with nine SQUID magnetometers, each 2.5 mm in diameter, arranged in a 3×3 square array with 2.75 mm between



each coil center. Three reference sensors, arranged at right angles to each other, are placed along the sensor array shaft, and the subject and sensor array sit inside a shielded box. In addition, an accelerometer is mounted on the machine to provide a vibration reference. A trigger pulse delivered by the audio system before each stimulus and recorded by the MEG system serves to align stimulus and response. The sensor array was placed in the same position relative to head features for all subjects (Fig. 1A), but no other anatomic coregistration was attempted, as the limited signal-to-noise ratio and small number of sensors prevent accurate source localization. Our aim was to characterize the time course of responses rather than their spatial characteristics.

Subjects. All experiments were performed under licenses granted by the United Kingdom Home Office in accordance with the United Kingdom Animal (Scientific Procedures) Act of 1986. Subjects were 17 adult male Duncan-Hartley guinea pigs; 8 animals were used for basic response characterization and 9 animals were used for experiments on response adaptation. All animals were anesthetised using 20% urethane (1.5g/kg body wt, single intraperitoneal injection) and 0.3 mg/ml buprenorphine (0.05 mg/kg body wt, single subcutaneous injection); 0.6 mg/ml atropine sulphate (0.2 ml, single subcutaneous injection) was also administered to reduce respiratory secretions. The state of the animal was monitored through assessment of the pedal withdrawal reflex and the use of a MouseOx vital sign monitor (STARR Life Sciences) to track breathing rate, O₂ saturation, and heart rate. Once the animal was anesthetised, its head was shaved and then placed into a custom head rest (Fig. 1A). The tube of a custom earpiece was inserted into the right ear just at the entrance to the auditory canal and then sealed into the outer ear using soft silicone ear plugs. The animal was then placed into the MEG machine, and the sensor array was positioned dorsally over the vertex of the skull (Fig. 1A) in an entirely noninvasive procedure. The plane of the sensor array was thus oriented parallel to cortical columns within the auditory cortex, which lies along the lateral surface of the brain in guinea pigs.

Guinea pigs, like other small rodents, are lissencephalic; that is, the cortical surface is smooth and lacking gyri, and cortical currents therefore tend to be radial to the skull surface. For a uniform spherical conductor, radial current dipoles produce no measurable magnetic field outside the sphere, as a result of the balance between primary and return currents (Baule and McFee 1965). However, the shape of the guinea pig brain differs significantly from a sphere, and primary currents may not be perfectly radial, so measurable magnetic fields may be present outside the head (Barth 1991). We positioned the MEG sensors on the dorsal surface of the skull, in a plane parallel to the expected direction of current flow in the auditory cortex, and were able to pick up magnetic fields produced by primary or return currents induced by auditory stimuli. Notably, we were able to obtain clear

AEFs using this noninvasive approach (cf. Barth 1991; Barth et al. 1986) without resorting to more invasive methods, as used in some previous studies (Barth and Sutherland 1988; Bowyer et al. 1999).

Auditory stimuli. Stimuli consisted of sequences of tone pips that alternated between two sound frequencies (Fig. 1B). The choice of stimulus conditions was limited by constraints specific to MEG recording. Transducers had to be placed outside the magnetically shielded box, and stimuli were therefore transmitted via tubing to the animal's ears, limiting their spectral range. Furthermore, a large number of repeats of each stimulus was needed to overcome magnetic noise, limiting the number of different stimulus conditions. Stimuli were synthesised in MATLAB (Mathworks) and played out using PureData (<http://puredata.info>) via ER-2 transducers (Etymotics), which were located in a magnetically shielded box outside the MEG machine and connected to the custom earpiece via ~25 cm of 1.6-mm-inner diameter polythene tubing. Sound levels were calibrated in situ with a microphone (40BF free-field microphone, G.R.A.S Sound & Vibration) inserted into the custom ear piece. Calibrations included a compensation for attenuation of the sound signal between the microphone and the eardrum, which was estimated before the experiments using a simulated ear canal. The frequency response characteristics of the transducers, combined with low-frequency filtering effects of the tubing, limited the range of effectively transmitted sound frequencies to ~0.5–4 kHz, which is at the lower end of the guinea pig hearing range.

A roving standard stimulus paradigm (Fig. 1B) (Haenschel et al. 2005) was used to achieve efficient yield of data for analysis of deviant and standard responses and to facilitate comparison with the growing number of studies in awake humans using this paradigm (e.g., Costa-Faidella et al. 2011; Cowan et al. 1993; Haenschel et al. 2005). Tone sequences were composed of alternating series of repeated tones. Tones were 30 ms in duration (with 5-ms cosine-squared rise/fall times), isochronously presented, and alternated between two different sound frequencies in each stimulus block (Fig. 1B). A block consisted of 92 repeats of the tone series at each of the 2 sound frequencies (hence, 183 frequency transitions). Each experiment involved the presentation of stimulus blocks with parameters chosen to optimize data collection either for analysis of basic characteristics of AEFs or for analysis of the reduction in amplitude of the evoked fields with tone repetition.

For basic response characterization, tone frequencies were separated by 0.25, 0.5, 1, or 2 octaves around a center frequency of 1.6 kHz. The number of tones in a series before a frequency transition (N) was always 4, and the interval between tone onsets [interonset interval (IOI)] was always 400 ms. Responses to these stimuli were used to analyze AEF characteristics, including waveform shape, extrema

Fig. 1. Brain responses to tone pips in the guinea pig, as measured noninvasively with small-animal magnetoencephalography (MEG). *A*: MEG experimental setup. *Left*, view of the small-animal MEG machine with the helium dewar visible on top of the recording chamber. *Middle*, close-up view of the recording chamber, with the adjustable platform for the animal below the extremity of the dewar containing the MEG sensors. *Right*, an anesthetised guinea pig with its head resting on the head holder and the dewar containing MEG sensors pressed lightly on the dorsal surface of the head. Plastic tubing held in place near the ears is attached to speakers outside the recording chamber, so that acoustic stimuli can be delivered directly into the auditory canal. *B*: in the roving standard paradigm, a series of tones of the same frequency and at the same interonset interval (IOI) is followed by a series at a new frequency separated by ΔF , with possibly a different IOI and number of tone repetitions in the series. The initial tone in each series (red) acts as a deviant stimulus compared with the standard stimuli of remaining tones in the series (blue). *C*: individual channel waveforms evoked by a 3.2-kHz tone. *Left*, mean raw waveform averaged over ~14,000 repeats; gray shading indicates bootstrapped SD in the mean (equivalent to SE here; bootstrap used for consistency with other analyses). *Middle*, waveform after time-shift principal components analysis (TSPCA), which removes environmental noise such as 50-Hz or machine-induced magnetic fields. *Right*, waveform after TSPCA and denoising source separation (DSS; see METHODS). The first DSS component (the most reliable linear combination of channels) was backprojected into the sensor space to produce the denoised auditory evoked field (AEF). *D*: population average AEF for the 3.2-kHz tone, averaged across all tone presentations and all 9 animals used for experiments of response adaptation. The amplitude was calculated as the root mean squared amplitude across sensors. The shaded region indicates a bootstrap estimate of 1 SD around the population mean (i.e., SE). The guinea pig AEF was characterized by three extrema, with latencies of 10–30 ms (c_{M20}), 25–75 ms (c_{M50}), and 100–175 ms (c_{M140}) relative to the stimulus onset (see METHODS). *E*: spatial variation in AEF for one animal, illustrated by backprojecting the first DSS component into the sensor space for all nine sensors. The color indicates waveform polarity; the arrangement of plots reflects the arrangement of the nine magnetometers in the sensor array. *F*: AEFs for responses to a 30-ms, 3.2-kHz tone pip from four different animals used for experiments of response adaptation. Responses are averaged across both standard and deviant conditions, with shading indicating bootstrapped SD of the mean. These results demonstrate the consistency of MEG responses both within and across animals.

latency, and the frequency dependence of extrema latency and amplitude.

For experiments on the reduction in AEF amplitudes with tone repetition, we fixed tone frequencies at 800 and 3.2 kHz (2-octave separation) to maximize sound frequency change within the constraints imposed by the frequency response of the MEG-compatible sound delivery system and hearing range of the guinea pig. We then systematically varied the time between transitions [interdeviant interval (IDI)] and N in a 2×2 (IDI = 1.6 or 3.2 s, $N = 4$ or 8) design. Previous studies in humans using roving standard stimuli have sometimes observed effects of increasing N even further, e.g., to 12 tones/transition (e.g., Costa-Faidella et al. 2011). Our decision to use either 4 or 8 tones/transition was dictated by the need to have enough transition events in each experiment to overcome the low signal-to-noise ratio of noninvasive MEG measurements in small animals.

Tone sequences used for experiments on the reduction in evoked field amplitudes therefore included tone series with four different possible temporal patterns (at each of the two possible alternating tone frequencies): 200-ms IOI, $N = 4$; 400-ms IOI, $N = 4$; 400-ms IOI, $N = 8$; or 800-ms IOI, $N = 4$. [Nominal IOIs were augmented by a small amount (1.14 ms) to ensure that power line interference components (50 Hz and harmonics) were not reinforced by trial averaging.] At every frequency transition in the tone sequence, the temporal presentation pattern for the next tone series was chosen randomly from among the four possible conditions, so that an equal number of each type of series would be presented in each hour. We aimed to collect a minimum of 6 h of data per subject, with more data collected if conditions permitted.

Data acquisition and analysis. MEG and reference data were collected using custom software provided by the Applied Electronics Laboratory (SQUIDLab). Sensor signals were band-pass filtered in hardware between 0.5 and 500 Hz and sampled at 1 kHz. Sampled signals were digitally high-pass filtered at 1 Hz, smoothed with a four-sample boxcar filter, and then separated into trials of either 350-ms duration (basic response analysis) or 175-ms duration (analysis of response reduction with tone repetition).

The aim of the data analysis was to extract the weak stimulus-evoked magnetic response from a combination of high-amplitude environmental and physiological noise. To achieve the highest possible signal-to-noise ratio in the processed data, we averaged signals across repeated trials and also applied three denoising techniques: outlier rejection, time-shift principal components analysis (TSPCA) (de Cheveigné and Simon 2007), and denoising source separation (DSS) (de Cheveigné and Parra 2014; Särelä and Valpola 2005) (Fig. 1C).

Outlier rejection is a standard procedure that is recommended before applying least-squares methods such as averaging, regression, or principal components analysis because these procedures are sensitive to large deviations from the mean. We removed outliers both before and after other denoising steps, such as TSPCA and DSS, since each denoising step revealed new outliers that were previously masked by noise. These successive outlier removal steps had little impact on final estimates of the MEG signal in most cases but were necessary to counteract the effects of occasional large signal glitches due to transient environmental noise.

TSPCA was applied to the recordings from each MEG channel separately. This denoising method effectively suppresses environmental noise, such as 50-Hz signals from electrical equipment (see de Cheveigné and Simon 2007 for details).

Recordings from different channels were then combined by applying DSS, a denoising technique that derives linear combinations of channels that optimize the signal with respect to a defined criterion, such as repeatability over trials or differentiation of stimulus conditions (de Cheveigné and Parra 2014; de Cheveigné and Simon 2008). DSS produces a set of mutually uncorrelated component signals, ordered by decreasing criterion score. For our analysis, we used the first DSS component, representing the linear combination of channel

signals with the highest possible signal-to-noise ratio. This first DSS component was projected back into sensor space to produce a set of denoised sensor waveforms (Fig. 1E), which we then averaged to obtain our best estimate of the cortical response (see APPENDIX: THE DENOISING PROCESS for full details). Thus, AEF used for all further analyses was the average of the denoised sensor waveforms obtained by backprojecting the first DSS component into sensor space.

The average over trials of this AEF waveform typically consisted of a series of three deflections. Adopting nomenclature similar to that used in human studies, we labeled these three extrema by their approximate latencies as cM20 , cM50 , and cM140 , where the subscript c is a species designator taken from the guinea pig genus name: *Cavia*. The value of AEF at each of these extrema was quantified as the most extreme value within a small temporal window around the reference latency (window bounds: 10–30 ms for cM20 , 25–75 ms for cM50 , and 100–175 ms for cM140). The relative polarities of these extrema are well defined, but the absolute polarities are not. (To infer the polarities of the source currents within the auditory cortex from the weighted sum of brain activity in the MEG signal, we would need precise knowledge of the position of the sensors relative to auditory cortex, a forward model specific to the guinea pig head, and the simplifying assumption of a dipolar source.)

The magnitude of AEF extrema usually decreased between the first and subsequent tones of a series (4 or 8 tones of the same frequency). For each extremum, the degree of AEF reduction was quantified using the reduction index (RI), which was defined as the distance in SDs between the observed AEF extremum amplitude for noninitial tones and mean AEF extremum amplitude that would be obtained under the null hypothesis of no reduction with tone repetition. This z -scored measure was used to assess the significance of the AEF reduction in individual subjects, since it took into account the noise level of the recording for each subject. To facilitate comparison with previous studies, we also analyzed the AEF reduction for each subject using the more conventional approach of normalizing the AEF extremum magnitude for noninitial tones by the AEF extremum magnitude for initial tones (see Fig. 3C).

Model. To quantify the time course of the AEF reduction with same-frequency tone repetition, we adapted a model previously used to describe short-term synaptic depression (Dayan and Abbott 2001). Similar models have recently been used to model the dependence of SSA in single neurons on tone frequency and probability (Taaseh et al. 2011). Here, we used a simpler version to address the specific question: how quickly does cM50 magnitude reduce with repetition of 3.2-kHz tones? We focused on cM50 magnitude because the signal-to-noise ratio for MEG measurements was consistently highest for this extremum; likewise, we considered only responses to 3.2-kHz tones in this analysis because the strongest MEG responses were evoked at this tone frequency.

Assuming an initial state of an extended period of silence, the cM50 magnitude to the first stimulus in a series (m_1) occurring at time t_1 has a value equal to the maximum cM50 magnitude (M). After any activity, the responsiveness of the system is immediately suppressed to a fraction $\alpha \in [0,1]$ of its previous responsiveness, which then recovers back to its baseline state with a time constant (τ). So, for the n th stimulus, cM50 magnitude m_n at time t_n can be defined as follows:

$$m_n = \alpha m_{n-1} + (M - \alpha m_{n-1})(1 - e^{-(t_n - t_{n-1})/\tau})$$

The value of M was estimated from the mean AEF amplitude for the initial tone in all 3.2-kHz tone series, aggregating across different IOI and N conditions. We divided the data into 10 parts and fit model parameters α and τ to 9/10 of the data from all IOI and N conditions using the simplex search method (Lagarias et al. 1998) with cross-validation on the remaining 1/10 of the data. This procedure was repeated 10 times, with disjoint subsets of the data used for cross-validation. Model parameters reported here are, for each subject, the average parameters obtained from the 10 cross-validated model fits.

RESULTS

The nine-sensor array in the small-animal MEG machine was positioned on the dorsal surface of the animal's head to detect signals arising from radial current flow in the laterally positioned auditory cortex (Fig. 1A). Data from each of the nine sensors were denoised (Fig. 1C) and linearly combined to obtain a representation of AEF that optimized the reliability of stimulus-evoked responses and differentiation of stimulus conditions (Fig. 1E; optimal linear combination of sensor signals shown backprojected onto different channels to indicate signal strength at each sensor location). We defined AEF to be this optimized estimate of the auditory evoked response (the first DSS component, backprojected into sensor space and averaged across sensors; see METHODS) and used this representation for all further analyses (Fig. 1, D and F, and subsequent figures).

Basic response characteristics. While AEF in response to a 30-ms tone pip varied in magnitude and in shape between individual subjects (Fig. 1F), three clearly defined extrema were consistent across subjects: two early ones sharing the same polarity and a later extremum of opposite polarity (Fig. 1D). (As shown in Fig. 1F, in some subjects, there was another early extremum of the same polarity as the late extremum, but in other subjects, this additional extremum was absent; since it was not present in the population average, we do not discuss it further here.) As explained in METHODS, we denoted the three reliable extrema by their approximate latencies as cM20 , cM50 , and cM140 .

Studies in humans have shown a similar overall AEF profile, with the latencies of the extrema approximately twice what we observe here. Auditory evoked potentials (AEPs) measured in other rodents [using electroencephalography (EEG)] also have extrema with comparable latencies (Ehlers et al. 1994; Sambeth et al. 2003; Siegel et al. 2003; Umbricht et al. 2004, 2005), although rodent AEPs exhibit additional, longer-latency components than reported here, and the shortest latency components may be reversed in polarity relative to other extrema (see DISCUSSION).

In humans, both the magnitudes and latencies of AEF extrema are known to be dependent on the frequency of the tone stimulus (Roberts et al. 2000). In guinea pigs, AEF extrema amplitudes increased in absolute magnitude with increasing tone frequency (Fig. 2, regressions for cM50 and cM140 significant at $P < 0.01$, regression for cM20 significant at $P < 0.05$), but there was no dependence of AEF extrema latencies on tone frequency (all regressions $P > 0.1$; data not shown). However, experimental time constraints and equipment considerations limited us to collecting data for only a small portion of the guinea pig hearing range, which extends from ~ 50 Hz to 50 kHz. It is possible that AEF extrema latencies might show frequency dependence over a larger frequency range, similar to the weak frequency dependence of AEF extrema latencies in humans (Roberts and Pöppel 1996).

AEF changes with tone repetition. To analyze changes in AEF waveforms with tone repetition, we focused on responses to tones at 3.2-kHz sound frequency, for which the AEF magnitude, and our statistical power to resolve changes, was highest. Within each series of repeated tones, the waveform shape of AEF remained relatively stable, but the latency of the latest of the extrema and the overall amplitude of all three extrema differed between the first tone after a frequency

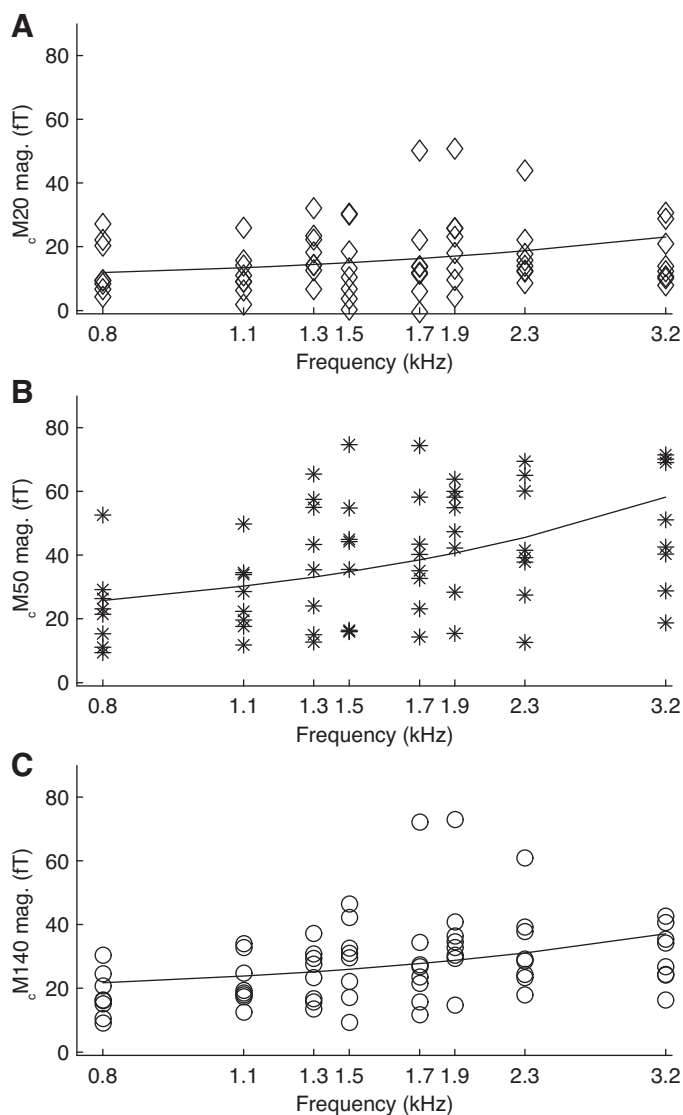


Fig. 2. Magnitudes of AEF extrema as a function of tone frequency. The magnitude (absolute value of response amplitude) of each of the AEF extrema increased with increasing frequency of the tone pip from 800 Hz to 3.2 kHz. Plots show data from all 8 animals used for basic response characterisation experiments, with linear regression lines (note that abscissa is logarithmic). A: cM20 ; linear regression $4.6 \text{ fT/kHz} + 8.2 \text{ fT}$, $p < 0.05$. B: cM50 ; linear regression $13.5 \text{ fT/kHz} + 15.0 \text{ fT}$, $p < 0.01$. C: cM140 ; linear regression $6.4 \text{ fT/kHz} + 16.6 \text{ fT}$, $p < 0.01$.

transition (deviant) and subsequent (standard) tones, especially at fast repetition rates (Fig. 3A).

Whereas there were no significant changes in extrema latency for cM20 or cM50 , the cM140 latency was longer for deviant than standard tones, particularly at the shortest IOI of 200 ms (Fig. 3B). At 200-ms IOI, we also observed a strong reduction in AEF amplitude with tone repetition for all three extrema (Fig. 3). To facilitate comparison with similar analyses in previous MEG studies, in Fig. 3C we show AEF extremum magnitude for later (standard) tones normalized by AEF extremum magnitude for initial (deviant) tones. Across subjects, this measure of the relative response to repeated versus initial tones was significantly < 1 for 200-ms IOI ($P < 0.01$ by Wilcoxon rank-sum test on medians). Similar results were obtained for 200-ms IOI using a z-scored measure (RI; see

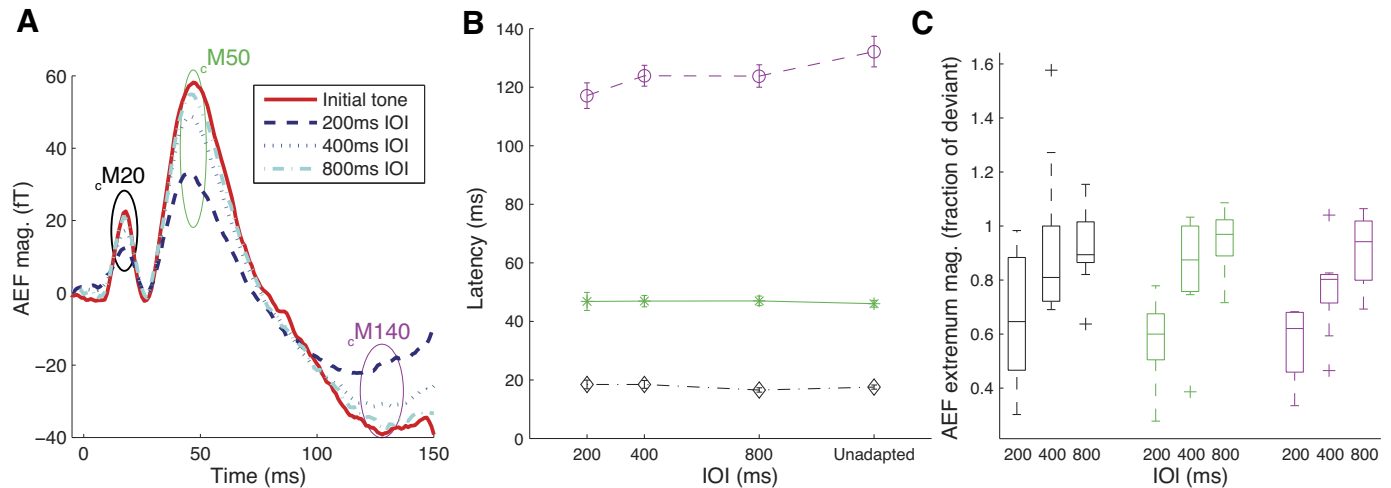


Fig. 3. Dependence of MEG responses to tones on IOI. **A:** population average AEFs for 3.2-kHz tones revealed that compared with responses to the initial tones, responses to later tones in a 200-ms IOI series were markedly reduced in amplitude. For tone series with 400- and 800-ms IOI, the degree of AEF reduction was considerably less. Ellipses indicate approximate positions of the extrema (black, M20 ; green, M50 ; and purple, M140). **B:** latencies of M20 and M50 did not vary significantly with IOI ($P > 0.1$ by repeated-measures ANOVA); however, there was a significant effect of IOI on latency of M140 ($P < 0.01$ by repeated-measures ANOVA). At faster IOIs, the latency of M140 was shorter for later tones than for initial (“unadapted”) tones in the sequences. **C:** box and whisker plots showing magnitudes of responses to repeated tones across subjects, for the three AEF extrema and for different IOI conditions. Response magnitude is quantified as the average AEF extremum magnitude for later tones in a series, normalized by AEF extremum magnitude for the initial (deviant) tone, to illustrate the degree of AEF reduction. For all three extrema, the amount of AEF reduction with tone repetition decreased with increasing IOI ($P < 0.01$ by repeated-measures ANOVA). This effect arose primarily from the AEF reduction with tone repetition at the fastest IOI, since only the 200-ms IOI condition produced a consistent reduction in AEF magnitude for later relative to initial tones ($P < 0.05$ for M50 and $P < 0.01$ for M140 with a similar trend at $P = 0.06$ for M20 by Wilcoxon rank-sum test for difference in medians at 200-ms IOI). See the reduction index analysis results in text for similar results obtained using a z -scored measure taking into account the signal-to-noise levels in recordings from different subjects.

METHODS) to take into account differences between subjects in the signal-to-noise level of recordings (RI > 2.5 : 5 of 9 subjects for M20 , 9 of 9 subjects for M50 , and 8 of 9 subjects for M140). However, for longer IOIs, reductions in extrema amplitude with tone repetition were neither significant across subjects (Fig. 3C) nor consistently observed in individual subjects. More precisely, at the intermediate IOI of 400 ms, only a subset of the subjects showed significant AEF reduction with tone repetition at 400-ms IOI (RI > 2.5 : 1 of 9 subjects for M20 , 5 of 9 subjects for M50 , and 5 of 9 subjects for M140); at the largest IOI of 800 ms, few subjects showed AEF reduction with tone repetition (0 of 9 subjects for M20 , 1 of 9 subjects for M50 , and 2 of 9 subjects for M140).

In principle, the AEF amplitude reduction with tone repetition shown in Fig. 3A could arise either from a reduction of the standard AEF response (e.g., adaptation) or from an augmentation of the deviant AEF response (e.g., a novelty effect) or both. If it were a novelty effect, we would expect the size of the deviant AEF response to increase with the time elapsed between transitions (IDI; Fig. 4A) or N (Fig. 4B). We therefore compared the deviant AEF magnitude between IDI = 1.6 and 3.2 s conditions and also between $N = 4$ and 8 conditions for each subject. For all three extrema and for most subjects, there were no significant differences in deviant AEF magnitude between IDI conditions or N conditions (Fig. 4C). (The only exceptions were as follows: two subjects, deviant M50 magnitude smaller at IDI = 1.6 s than IDI = 3.2 s, $P < 0.01$; one subject, deviant M140 weakly dependent on N , $P < 0.05$; and one subject, deviant M140 weakly dependent on IDI, $P < 0.05$.) Moreover, there was no significant change in deviant extremum latency for any of the extrema or conditions (Fig. 4D). Therefore, overall, we did not observe a large or consistent dependency of deviant AEF response on either N or IDI,

suggesting that novelty effects were minimal for the stimulus parameters tested.

Dependency of AEF reduction on IOI. To quantify the dependency of AEF reduction on IOI, we fit a model based on a widely used mathematical description of synaptic depression (see METHODS) with two parameters: the degree of responsiveness immediately after a tone presentation ($\alpha \in [0,1]$) and τ for the recovery of responsiveness between tone presentations. We fit the model only to M50 data for repeated 3.2-kHz tones, which produced the strongest and most reliable responses. For M20 , the responses were weak for several subjects, making for unreliable fits; for M140 , the latency shift was not consistent with the model’s assumption of a simple scaling of the response. We tested two versions of the model, one in which both τ and α were fit to the data and another in which only τ was fit and α was fixed to 0. There were no significant differences in cross-validation performance between the two models (data not shown), suggesting minimal cumulative effect of tone repetitions after the second tone in a series. We were therefore able to simplify the model by fixing α to 0 and fitting only the τ parameter. Model fits produced τ estimates for recovery from depression with a median across animals of 251 ms and 25% and 75% quartiles of 167 and 833 ms, respectively. These τ values are comparable to the duration of the IOIs themselves, again implying little cumulative effect of tone repetition and rapid recovery between tone presentations.

Figure 5A shows the reduction in M50 magnitude with tone repetition as a function of IOI. These data demonstrate that between the first tone and later tones in a series, the M50 magnitude drops by nearly 50% for 200-ms IOI but $<20\%$ for 400-ms IOI and $<10\%$ for 800-ms IOI. These data are consistent with the short τ estimates obtained from model fits. In fact, the predicted population mean M50 magnitude based on

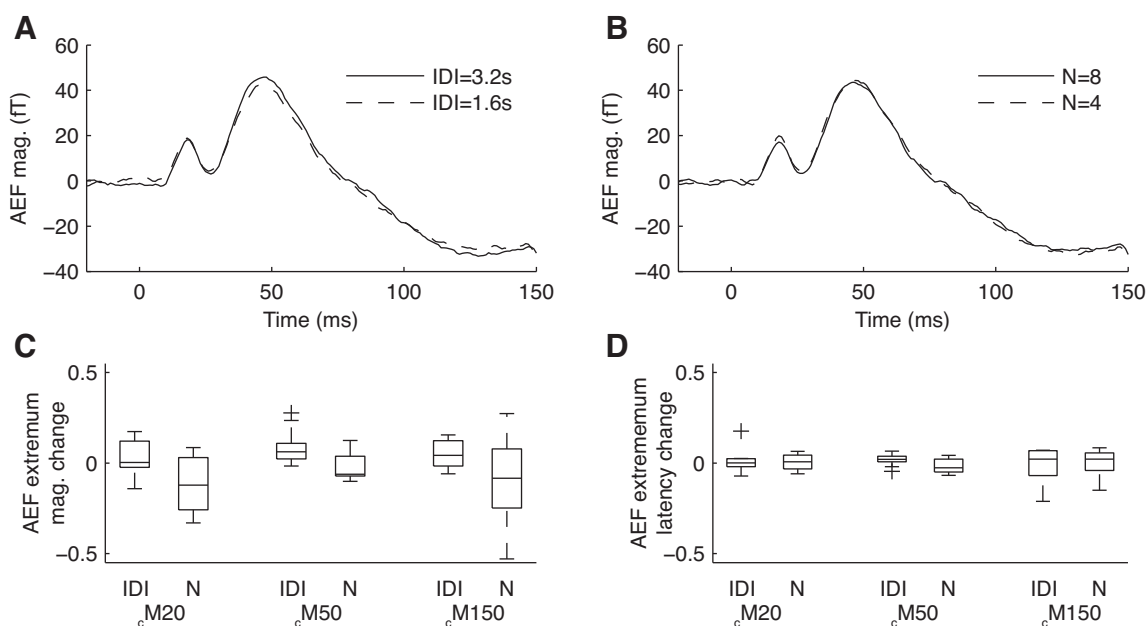


Fig. 4. Deviant AEF response shows no consistent dependence on either interdeviant interval (IDI) or length of preceding tone series (N). Deviants were separated by one of two IDIs (1.6 or 3.2 s) and one of two possible tone series lengths ($N = 4$ or 8). *A* and *B*: population grand averages of the deviant responses for the two different IDI (*A*) or N (*B*) conditions showed little difference. *C*: change in deviant response magnitude between IDI or N conditions for each of the three AEF extrema; more positive values signify a larger-magnitude AEF for 3.2-s IDI or $N = 8$ conditions, respectively. There were no significant changes in deviant extrema magnitudes between either IDI or N conditions across subjects (by Wilcoxon rank-sum test) nor in most individual subjects (see text). *D*: change in deviant response latency between IDI or N conditions for each of the three AEF extrema; more positive values signify a longer latency for 3.2-s IDI or $N = 8$ conditions, respectively. We observed no significant differences in extrema latency between any of the conditions for any extrema, either overall or in individual subjects.

the best-fit depression models for each subject (solid line in Fig. 5*A*) slightly overestimates the degree of AEF reduction at larger IOIs (note offset between solid line and data), suggesting that the recovery from successive tone presentations may actually be a faster process than the simple exponential recovery in the model.

We wondered if the relatively high noise levels in our guinea pig MEG data could have obscured detection of longer τ values like those reported in comparable human studies, perhaps because only large changes in $cM50$ amplitude with tone repetition would have been resolvable. To find out, we estimated the resolvability of AEF reductions for each of our subjects, by calculating the minimum percent reduction in $cM50$ amplitude that could have been resolved at $P < 0.01$ for recordings from each animal, given the $cM50$ amplitude for the first tones in each tone series and the variance of the signal. There was a large amount of variation between animals in the minimum resolvable $cM50$ reduction (range: 15–43%). Importantly, however, estimated τ values for AEF reduction with tone repetition were short even for subjects for which the minimum resolvable $cM50$ reduction was smallest (Fig. 5*B*). Of particular note is the fact that the minimum resolvable $cM50$ reduction was $<25\%$ in six of nine subjects. In a human study (Briley 2011), AEF reductions of 25% have been observed at IOIs of 1 s; therefore, we conclude that we should have been able to detect comparably long timescales for AEF reduction with tone repetition in the guinea pig if present.

Effects of the number of tone repetitions. The fact that τ values of the model fits were on the order of the smallest IOIs used in this study raises the possibility that the $cM50$ reduction with tone repetition might have been largely complete after a single repetition (i.e., two tone presentations) and that effects

of the length of the series of repeated tones might be minimal. This conclusion was confirmed by direct comparison of $cM50$ amplitudes between AEFs for the second and last (i.e., either fourth or eighth) tones in the tone series (Fig. 6). In no subjects was there any condition in which we observed a significant difference in AEF magnitude across the length of the tone series ($P > 0.05$ by t -test with Holm-Bonferroni correction). Thus, at least for the acoustic stimuli used in this study, there was no significant effect of the number of repeated tones on AEF reduction with tone repetition in the guinea pig.

In theory, optimizing the signal-to-noise ratio of the difference between responses to first and subsequent tones, as we did during the denoising process (see METHODS), might conceivably attenuate differences between responses to later tones. To address this concern, we modified the denoising process to optimize the difference between responses to second and subsequent tones (ignoring all responses to first tones; see METHODS) and repeated the previous analysis shown in Fig. 6. Again, we found no difference in $cM50$ amplitudes between AEFs for the second and last tones ($P > 0.05$ by t -test with Holm-Bonferroni correction). This additional analysis supports the conclusion that AEF reduction with tone repetition was essentially complete by the second tone in the repeated series.

Comparison with MMN-like response in humans. For comparison with MMN-like responses detected in comparable studies of awake human subjects, Fig. 7 shows grand-average (cross-trial and population) AEFs for the IOI = 400 ms condition plotted as for human data in Fig. 2*A* of Costa-Faidella et al. (2011): responses to standard (second and later) tones (Fig. 7*A*), responses to deviant (first) tones (Fig. 7*B*), and the difference between responses to deviant and standard tones

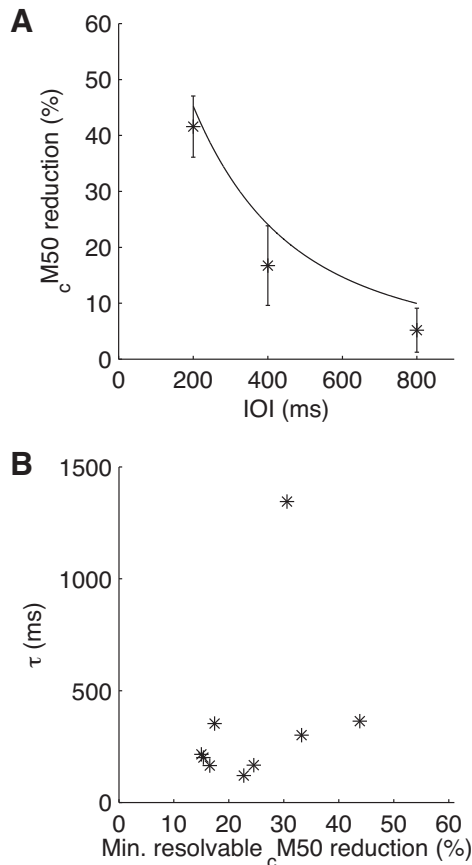


Fig. 5. Mathematical modeling of AEF reduction with tone repetition. *A*: reduction in $cM50$ magnitude for repeated versus initial tones in tone series plotted as a function of IOI along with the mean across the population of the predictions from the depression model (solid line). *B*: time constant (τ) from the model fits plotted against the minimum resolvable reduction in $cM50$ (a measure of noise level in the recordings) for each subject. Short τ values were obtained even in subjects for which the minimum resolvable $cM50$ reduction was $<25\%$ (6 of 9 subjects), which would have been sufficient to resolve event-related potential reductions at 1,000-ms IOI in human studies (Briley et al. 2011).

(Fig. 7C). Our results in anesthetised guinea pigs show many similarities to those measured in awake humans using a similar paradigm. Costa-Faidella et al. (2011) examined responses to standards and deviants in a roving standard paradigm (with 25 frequencies between 880 and 2,921 Hz) using tone series of length 3, 6, or 12. In that study, subtracting the standard response from that of the deviant revealed a negative MMN-like response that peaked after the N100 onset response (at the time of its downward slope); however, there was no effect of tone series length on responses to either standard or deviant tones except for very long series (12 tones) (see also Haenschel et al. 2005). Consistent with those findings in humans, the guinea pig MEG data revealed a grand-average difference waveform that peaked after, rather than at the same time as, $cM50$, and there was no effect of tone series length ($N = 4$ vs. 8) on responses to either standard or deviant tones. The latency shift in the deviant-standard difference waveform, although comparatively small (7.9 ms), was significant at the population level for both $N = 4$ and 8 tone series lengths ($P < 0.05$ for grand averages by bootstrap; not significant in individual subjects).

We have no evidence that $cM50$ is functionally homologous to N100; moreover, the degree to which the MMN-like response observed in roving standard paradigms constitutes a bona fide novelty response is not clear (Nelken and Ulanovsky 2007). Nevertheless, the present pattern of results raises the possibility that, rather than representing an exogenous response, the late MMN-like deflection that we observed might arise from the same low-level adaptive processes that produce a shorter $cM140$ latency for standard (repeated) relative to deviant (initial) tones.

DISCUSSION

Here, we have presented evidence that 1) AEFs with deflections resembling those observed in human MEG studies can be detected noninvasively in rodents using small-animal MEG; 2) AEF amplitudes in the anesthetised guinea pig reduce rapidly with tone repetition, and this AEF reduction is largely complete by the second tone in a repeated series; and 3) differences between responses to the first (deviant) and later (standard) tones after a frequency transition resemble those previously observed in awake humans using a similar roving standard stimulus paradigm.

Small-animal MEG. Standard whole-head MEG machines designed for human use have previously been used to characterize auditory and somatosensory evoked fields in the macaque monkey (Zhu et al. 2009; Zurner et al. 2010). However, there have been no previous studies of sensory or cognitive processing using MEG in rodents, because small-animal MEG is a relatively novel technology. Small-animal MEG machines have been used to study the generative mechanisms of the MEG signal (e.g., Okada et al. 1997, 1999) and to examine large-scale changes in the overall cortical state, such as spreading depression (e.g., Eiselt et al. 2004; Gardner-Medwin et al. 1991) or epileptic seizures (e.g., Barth et al. 1984). All previous incarnations of the technology have included some aspect of the preparation beyond anesthesia that is not comparable to the use of MEG in human sensory studies: for example, a surgically invasive (e.g., Nowak et al. 1999) or in vitro (e.g., Okada et al. 1997) approach, a focus on very low-frequency activity (e.g., Eiselt et al. 2004; Gardner-Medwin et al. 1991), or the use of a single sensor (e.g., Barth et al. 1984). With the advent of a compact multisensor MEG array (Miyamoto et al. 2008) and with the aid of advances in denoising methods (de Cheveigné and Parra 2014; de Cheveigné and Simon 2007; Särelä and Valpola 2005), we have been able to perform a sensorineural MEG study on par with previous human MEG studies and existing small-animal EEG studies (e.g., Kraus et al. 1994; Lazar and Metherate 2003; Umbricht et al. 2005).

Comparison with EEG. As an experimental technique for studies of auditory function, small-animal MEG has several advantages over EEG. MEG is appealing for comparative physiology: magnetic fields are less distorted by the skull and scalp than electrical fields (Okada et al. 1999), so MEG signals are less susceptible to species-specific distortions due to gross morphological differences in head shape. Moreover, small-animal MEG is a direct analog to human MEG, which is commonly used for auditory cortex studies because the positioning of the auditory cortex in the human brain makes evoked magnetic fields relatively easy to record at the skull surface. Small-animal MEG measurements are also less invasive than

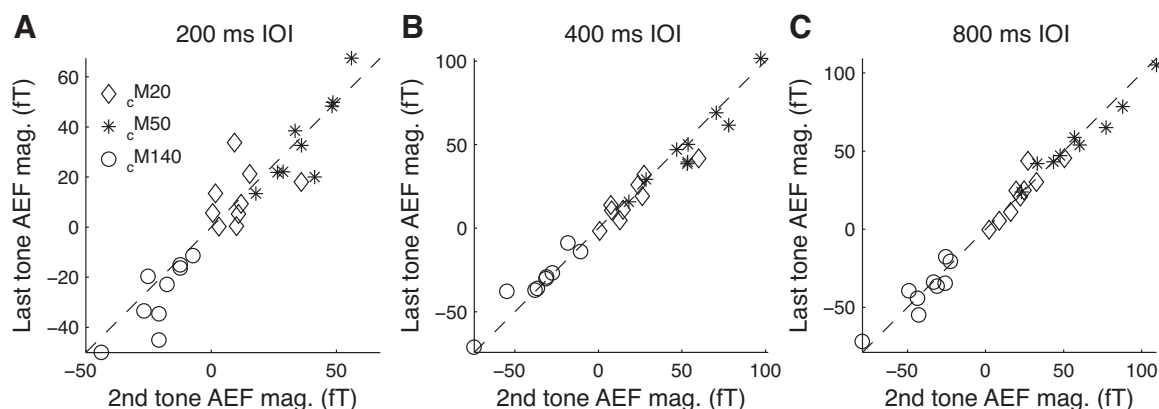


Fig. 6. No dependence of AEF reduction with tone repetition on the number of repeated tones. The magnitudes of the AEF at μ M20 (diamond), μ M50 (star), and μ M140 (circle) for the last tones in all tone series (y-axis) are plotted against the AEF magnitudes for second tones in all tone series (x-axis) for each subject; dashed line indicates equal magnitude (slope=1). The last tone was the eighth tone for 200 ms IOI (A) and 400 ms IOI (B) series, and the fourth tone for 800 ms IOI series (C). There was no significant difference between the AEF extrema magnitudes for the second versus last tones in any of the stimulus conditions, for any of the subjects (*t*-test with Holm-Bonferroni correction, $p > 0.05$.)

most small-animal EEG measurements, which typically involve the use of subdural or at least subdermal electrodes (e.g., Lazar and Metherate 2003). This advantage is offset by a greater susceptibility of MEG to environmental noise, for which we compensate here with a relatively sophisticated denoising process. One specific disadvantage of MEG relative to EEG is that the superconducting MEG sensors (SQUIDS) require cooling with liquid helium, which is a limited natural resource with a volatile global market (Nuttall et al. 2012).

In general, the AEF waveforms that we measured noninvasively in guinea pigs were similar in shape to AEPs measured in other rodents using invasive EEG recording techniques (Ehlers et al. 1994; Sambeth et al. 2003; Siegel et al. 2003; Umbricht et al. 2004, 2005), with polarity reversed from that typically used to display AEPs (as is conventional also for many human MEG studies). The strong μ M50 AEF extremum we observe in guinea pigs most likely corresponds to the large negative extremum that occurs at a latency of 40–80 ms in the rat AEP (Sambeth et al. 2003) and 30–50 ms in the mouse AEP (Umbricht et al. 2004) and that is considered a possible analog of the human N100. Similarly, the μ M140 extremum of opposite polarity after μ M50 in the guinea pig may correspond to the positive extremum in rat and mouse AEPs with latency 80–150

ms in rats (Sambeth et al. 2003) and 70–120 ms in mice (Umbricht et al. 2004); this wave is considered a possible analog of human P200. An early component like μ M20 in guinea pig AEF is also sometimes observed in rat and mouse AEPs at similar latencies. This early extremum, when it appears, usually has polarity opposite to that of the large N100-like extremum in rat and mouse AEPs (Sambeth et al. 2003; Siegel et al. 2003; Umbricht et al. 2004), while, in most cases, μ M20 had the same polarity as μ M50 in guinea pig AEF. In addition, longer-latency components that are sometimes evident in rodent AEPs were not detected in guinea pig AEFs. These differences in the characteristics and visibility of the weaker extrema in guinea pig AEF versus rat and mouse AEPs might reflect species differences or differences in the measurement techniques. However, the features of rodent AEPs that are most consistent across EEG studies were reliably observed here in guinea pig AEFs, providing confidence that the recorded MEG signals arise from similar auditory cortical sources as EEG signals.

Effects of tone repetition on AEF. Our finding that reduction of the μ M50 magnitude occurs only for short IOIs (Fig. 3) appears to be at odds with results of several previous experiments in humans and animals. Paradigms designed to probe

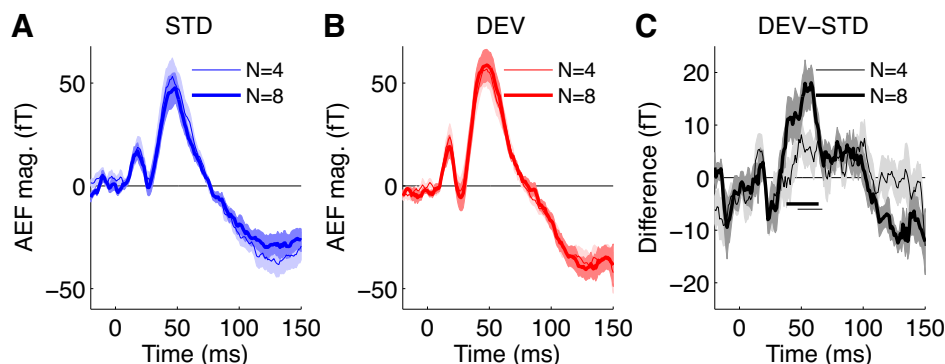


Fig. 7. Deviant-minus-standard differences in grand-average AEFs resemble those observed using similar stimulus paradigms in awake humans (cf. Costa-Faidella et al. 2011). A–C: grand-average AEFs for standard (A) and deviant (B) tones and the deviant-minus-standard difference waveform (C) for 400-ms IOI and either $N = 4$ (thin) or 8 (thick) conditions. Shaded regions indicate 1 SD of the bootstrap estimate of the SE (overlapping for $N = 4$ and 8 conditions). Grand-average AEFs for deviant tones differed significantly from grand-average AEFs for standard tones in both $N = 4$ and 8 conditions (with no significant differences between $N = 4$ and 8 responses). The horizontal bars indicate the region near 50-ms latency where the waves are significantly different at $P < 0.05$ for the $N = 4$ and 8 conditions. For comparison with a very similar analysis performed on AEFs from awake humans, see Fig. 2A in Costa-Faidella et al. (2011).

stimulus-specific adaptation in human MEG can elicit effects with interstimulus intervals of 1 s or longer (e.g., Briley 2011; Salminen et al. 2009), whereas in our data, only the 200-ms IOI tone series reliably generated observable amounts of AEF reduction. A comparable EEG study in rats (Lazar and Metherate 2003) also reported a significant reduction to ~55% of the unadapted response at 500-ms IOI [and single-neuron studies of SSA in cats and rats have reported effects even at 1- or 2 s-IOI (e.g., Ulanovsky et al. 2004; Antunes et al. 2010)]. It does not seem likely that the dependence on IOI was confounded by train length; whereas all of the 200-ms IOI series had eight tones, for 400-ms IOI we had an equal number of series with four or eight tones, and we saw no effect of series length there (Fig. 6).

Possible explanations for this apparent discrepancy between present and previous results include differences in species, stimulation paradigm [roving standard versus oddball paradigm (see Bäuerle et al. 2011)], and stimulus characteristics [e.g., use of tone frequencies at the low-frequency end of the animal's hearing range here due to technical limitations of the small-animal MEG setup versus tone frequencies in the middle of the hearing range (Lazar and Metherate 2003)]. A fourth possibility is that the adaptation of the MEG signal we recorded in the guinea pig was driven primarily by subcortical rather than cortical processes. However, our analysis of AEF reduction was conducted on μ M50, and the most likely analog of this extremum in human AEF is M100, which is thought to originate in primary and association cortices (Papanicolaou et al. 1990; Rogers et al. 1990). Moreover, guinea pig μ M50 is clearly similar to rat P2 analyzed in Lazar and Metherate (2003), both in timing and polarity relative to other components of the rat AEP; Lazar and Metherate (2003) found a substantial reduction in P2 with tone repetition at 500-ms IOI.

Effects of the number of tone repetitions. In line with the observation of strong AEF reduction only at the shortest IOIs, we also found that AEF reduction was essentially complete after a single tone repetition. This result is consistent with findings from human MEG studies (Budd et al. 1998; Costa-Faidella et al. 2011; Haenschel et al. 2005; Rosburg et al. 2010; Soros et al. 2009), where a dependence of the AEF reduction on tone series length was usually observed for long, but not short, tone series. Both Haenschel et al. (2005) and Costa-Faidella et al. (2011) reported strong effects of tone series length only when the comparisons included tone series of length ≥ 12 , whereas studies that used shorter series reported no effect (Budd et al. 1998; Rosburg et al. 2010). Similarly, in our data, the differences between AEFs evoked by four- and eight-tone series were not significant (Figs. 4 and 7), but it is possible that longer series might have revealed an effect.

Differences between deviant and standard AEFs. We found no reliable dependence of deviant AEF on stimulus history. Thus, it would appear that the observed dependence of the deviant-standard difference response on the structure of the stimulus is dominated by changes in standard AEF relative to deviant AEF. Human studies using the roving standard paradigm have reached similar conclusions (Costa-Faidella et al. 2011; Cowan et al. 1993; Haenschel et al. 2005). Apparently consistent with our work, evoked potential studies in the anesthetized rat (Lazar and Metherate 2003) and mouse (Umbrecht et al. 2005) reported no differences in the response between deviant tones in a classic oddball paradigm and a

“deviant-alone” control in which the standard tones are effectively replaced with silence, and those authors thus concluded that there was no evidence for change detection (as reflected by an increase in deviant AEF amplitude). Nelken and Ulanovsky (2007) argued that such controls are overly strict and suggested instead a “many-standards” control. However, results with such controls have proven ambiguous, with some reporting clear changes relative to the oddball-deviant model (Nakamura et al. 2011) and some reporting no effect (Fishman and Steinschneider 2012); recent evidence suggests that the many-standards control is extremely sensitive to the range over which the standards are distributed (Taaseh et al. 2011). It is also possible that the isochronous tone series and roving standard stimulus design used here and in previous human studies might fail to produce changes in the deviant response that would be evoked by more substantial alterations in stimulus statistics (Yaron et al. 2012).

The latency of the peak of the deviant-minus-standard difference waveform (Fig. 7) was clearly distinct from the latency of the extrema of AEF, as is the case for responses labeled as MMN in previous human studies [although the latency shift is larger in awake humans for some stimulus paradigms (Kretschmar and Gutschalk 2010; Näätänen et al. 1989; Winkler et al. 1997) compared with others (Costa-Faidella et al. 2011; Haenschel et al. 2005)]. MMN-like responses measured in local field potentials and current source densities in the awake rat and macaque also appear to display similar or larger latency shifts (Fishman and Steinschneider 2012; Javitt et al. 1994; von der Behrens et al. 2009). This temporal shift is considered one of the key pieces of evidence in support of the idea that MMN is generated by a novelty-driven process distinct from the generators of N100 and other components of AEP (Näätänen et al. 2005). However, the fact that we observed a delay in the latency of the difference waveform in our data, even though we found no other evidence for changes in the deviant response, suggests that such latency shifts may not arise from brain processes related to the novelty of the deviant response. May and Tiitinen (2010) have argued that the temporal separation between the peak of the difference response and the extrema of deviant or standard responses might in fact be due to variability in the latency of N100; in our data, the most obvious explanation arises from the reduction in the latency of μ M140 for second and later tones (Fig. 3). These data raise the possibility that MMN-like latency shifts can arise through differential effects of tone repetition on the latency of early versus late deflections in the tone-evoked brain response. In any case, the remarkable similarity between the results obtained in anesthetized guinea pigs and awake humans using a similar stimulus paradigm (Costa-Faidella et al. 2011) suggests that the effect is generated by low-level, automatic mechanisms, independent of conscious awareness.

Possible effects of anaesthesia. One major difference between this work in guinea pigs and MEG studies in humans is that the guinea pigs were anesthetized (with urethane), whereas human MEG experiments are more often performed in awake subjects. The brain states evoked by urethane anesthesia are thought to be very similar to those evoked by sleep (Clement et al. 2008). Previous studies in humans have indicated that the MMN response is reduced under anesthesia (Simpson et al. 2002, but see Koelsch et al. 2006) and during slow-wave sleep (Csépe et al. 1987), and the magnetic counterpart of

MMN is also known to be attenuated by anticholinergic drugs (Pekkonen et al. 2001), such as the atropine administered here to reduce bronchial secretions in anaesthetised animals. Therefore, it is possible that the deviant-standard difference responses we recorded in anaesthetised, atropine-treated guinea pigs were weaker than those that would be obtained in awake animals. On the other hand, it should be noted that SSA has been repeatedly demonstrated and most often characterized in urethane-anaesthetised animals (Antunes et al. 2010; Duque et al. 2012), and, therefore, anaesthesia does not undermine the validity of our results regarding SSA. Indeed, the fact that we observed differences between responses to deviant and standard tones in the anaesthetised guinea pig that resemble differences previously described as MMN in awake humans strengthens our conclusion that MMN-like responses can arise from low-level adaptive processes independent of conscious awareness.

APPENDIX: THE DENOISING PROCESS

To achieve the highest possible signal-to-noise ratio for the stimulus-evoked magnetic response, we averaged signals across repeated trials, as in most studies, and applied three additional denoising techniques: outlier rejection to ensure that transient environmental noise did not bias our estimates of mean evoked fields; time-shift principal components analysis (TSPCA; de Cheveigné and Simon 2007) to remove environmental noise; and denoising source separation (DSS; Särelä and Valpola 2005; de Cheveigné and Parra 2014) to derive the linear combination of channels that provided the most reliable estimate of the evoked signal that differed between stimulus conditions.

Outlier rejection was performed at multiple stages in the denoising process, since each denoising step revealed new outliers that were previously masked by noise. In the first stage, performed on the raw data from each channel, trials with clipping on more than 2% of samples on any channel (including reference sensors) were discarded, as were trials that differed from the average over trials by more than 2 standard deviations. In the second stage, performed on the processed data following TSPCA (see below), trials deviating more than 1.5 standard deviations from the average TSPCA-transformed signal across trials were discarded. The third stage of outlier rejection was performed on the DSS component representing the most reliable stimulus-dependent signal that could be obtained from a linear combination of data from the nine MEG sensors (see below). Outliers in this stage were defined as trials in which this DSS component deviated by more than 2 standard deviations from its average across trials. Overall, typically 20% of trials were discarded, leaving at least 1000 trials per stimulus condition.

TSPCA was applied to the recordings from each channel to suppress environmental noise recorded on the reference sensors. TSPCA projects out magnetic fields recorded from the reference sensors, with time shifts to compensate for any convolutional mismatch between reference and main sensors.

The TSPCA-transformed data from all nine MEG sensors was then combined using the DSS procedure, to derive the linear combination of channels that optimised the reliability of stimulus-evoked responses and their differentiation across stimulus conditions. We first applied DSS with a reliability constraint, to obtain the linear combination of channels that optimised the reliability of stimulus-dependent activity. The first DSS component from this optimisation process was used for the final stage of outlier rejection, to identify and exclude trials in which the estimate of stimulus-dependent signal deviated significantly from the mean across repeated trials.

After the final outlier removal step, the DSS algorithm was applied once more, this time to optimise the *difference* between the response

to the first tone and subsequent tones in a series. Specifically, for each condition (first or subsequent) we subtracted from each trial the average over all trials of the *other* condition. These data were then submitted to DSS to find the linear combination of channels for which this difference was most reliable. The weights obtained in this way were applied uniformly to all the data of both conditions. Normalising this component, and multiplying by the RMS over sensors of its associated sensor-space projection, provides our best estimate of the magnetic field associated with the adaptation-related cortical response. (As a control, we also used a variation of the above procedure in which we replaced the first tone by the second tone, comparing it to the average over all trials from third or later tones in the series; see Results.) The DSS algorithm provides additional optimised components orthogonal to the first, but in these experiments, for all subjects, only a single component of the DSS displayed adaption-related responses. We therefore confined our analysis to that component alone.

ACKNOWLEDGMENTS

The authors acknowledge the pioneering contributions of Hisashi Kado to the development of the small-animal MEG machine used in this work and major role in arranging the collaboration between University College London (UCL) and the Kanazawa Institute of Technology to bring it to London. The authors also thank Gen Uehara, Yoshiaki Adachi, Jun Kawai, and Masakazu Miyamoto from the Kanazawa Institute of Technology for expert technical help with the small-animal MEG machine. Additional technical support was provided by Duncan Farquardt (UCL).

GRANTS

This work was supported by Biotechnology and Biological Sciences Research Council Grant BB/H006958/1 and a Travel Award from the Royal Society as well as École Normale Supérieure Grants ANR-10-LABX-0087 IEC and ANR-10-IDEX-0001-02 PSL*.

DISCLOSURES

No conflicts of interest, financial or otherwise, are declared by the author(s).

AUTHOR CONTRIBUTIONS

Author contributions: G.B.C., M.C., A.d.C., and J.F.L. conception and design of research; G.B.C. and J.F.L. performed experiments; G.B.C. and A.d.C. analyzed data; G.B.C., M.C., A.d.C., and J.F.L. interpreted results of experiments; G.B.C. and A.d.C. prepared figures; G.B.C. and M.C. drafted manuscript; G.B.C., M.C., A.d.C., and J.F.L. edited and revised manuscript; G.B.C., M.C., A.d.C., and J.F.L. approved final version of manuscript.

REFERENCES

- Antunes FM, Nelken I, Covey E, Malmierca MS. Stimulus-specific adaptation in the auditory thalamus of the anaesthetized rat. *PLoS ONE* 5: e14071, 2010.
- Ayala YA, Malmierca MS. Stimulus-specific adaptation and deviance detection in the inferior colliculus. *Front Neural Circuits* 6: 89, 2012.
- Barth DS. Empirical comparison of the MEG and EEG: animal models of the direct cortical response and epileptiform activity in neocortex. *Brain Topogr* 4: 85–93, 1991.
- Barth DS, Sutherling W, Beatty J. Fast and slow magnetic phenomena in focal epileptic seizures. *Science* 226: 855–857, 1984.
- Barth DS, Sutherling W. Current source-density and neuromagnetic analysis of the direct cortical response in rat cortex. *Brain Res* 450: 280–294, 1988.
- Barth DS, Sutherling W, Beatty J. Intracellular currents of interictal penicillin spikes: evidence from neuromagnetic mapping. *Brain Res* 368: 36–48, 1986.
- Baule G, McFee R. Theory of magnetic detection of the heart's electrical activity. *J Appl Phys* 36: 2066–2076, 1965.
- Bäuerle P, von der Behrens W, Kössl M, Gaese BH. Stimulus-specific adaptation in the gerbil primary auditory thalamus is the result of a fast

- frequency-specific habituation and is regulated by the corticofugal system. *J Neurosci* 31: 9708–9722, 2011.
- Boly M, Garrido MI, Gosseries O, Bruno MA, Boveroux P, Schnakers C, Massimini M, Litvak V, Laureys S, Friston K.** Preserved feedforward but impaired top-down processes in the vegetative state. *Science* 332: 858–862, 2011.
- Bowyer SM, Okada YC, Papuashvili N, Moran JE, Barkley GL, Welch KM, Tepley N.** Analysis of MEG signals of spreading cortical depression with propagation constrained to a rectangular cortical strip: I. Lissencephalic rabbit model. *Brain Res* 843: 71–78, 1999.
- Briley PM.** *Disentangling the Effects of Stimulus Context on Auditory Responses Using Electroencephalography* (PhD thesis). Nottingham: Univ. of Nottingham, 2011.
- Budd TW, Barry RJ, Gordon E, Rennie C, Michie PT.** Decrement of the N1 auditory event-related potential with stimulus repetition: habituation vs. refractoriness. *Int J Psychophysiol* 31: 51–68, 1998.
- Clement EA, Richard A, Thwaites M, Ailon J, Peters S, Dickson CT.** Cyclic and sleep-like spontaneous alternations of brain state under urethane anaesthesia. *PLOS ONE* 3: e2004, 2008.
- Costa-Faidella J, Baldeweg T, Grimm S, Escera C.** Interactions between “what” and “when” in the auditory system: temporal predictability enhances repetition suppression. *J Neurosci* 31: 18590–18597, 2011.
- Cowan N, Winkler I, Teder W, Näätänen R.** Memory prerequisites of mismatch negativity in the auditory event-related potential (ERP). *J Exp Psychol Learn Mem Cogn* 19: 909–921, 1993.
- Csépe V, Karmos G, Molnár M.** Evoked potential correlates of stimulus deviance during wakefulness and sleep in cat—animal model of mismatch negativity. *Electroencephalogr Clin Neurophysiol* 66: 571–578, 1987.
- Dayan P, Abbott LF.** *Theoretical Neuroscience: Computational and Mathematical Modeling of Neural Systems*. Cambridge, MA: MIT Press, 2001.
- de Cheveigné A, Simon JZ.** Denoising based on time-shift PCA. *J Neurosci Methods* 165: 297–305, 2007.
- de Cheveigné A, Simon JZ.** Denoising based on spatial filtering. *J Neurosci Methods* 171: 331–339, 2008.
- de Cheveigné A, Parra LC.** Joint decorrelation, a versatile tool for multi-channel data analysis. *Neuroimage* 98: 487–505, 2014.
- Duque D, Pérez-González D, Ayala YA, Palmer AR, Malmierca MS.** Topographic distribution, frequency, and intensity dependence of stimulus-specific adaptation in the inferior colliculus of the rat. *J Neurosci* 32: 17762–17774, 2012.
- Ehlers CL, Kaneko WM, Robledo P, Lopez AL.** Long-latency event-related potentials in rats: effects of task and stimulus parameters. *Neuroscience* 62: 759–769, 1994.
- Eiselt M, Giessler F, Platzek D, Hauelsen J, Zwiener U, Röther J.** Inhomogeneous propagation of cortical spreading depression—detection by electro- and magnetoencephalography in rats. *Brain Res* 1028: 83–91, 2004.
- Farley BJ, Quirk MC, Doherty JJ, Christian EP.** Stimulus-specific adaptation in auditory cortex is an NMDA-independent process distinct from the sensory novelty encoded by the mismatch negativity. *J Neurosci* 30: 16475–16484, 2010.
- Fishman YI, Steinschneider M.** Searching for the mismatch negativity in primary auditory cortex of the awake monkey: deviance detection or stimulus specific adaptation? *J Neurosci* 32: 15747–15758, 2012.
- Fruhstorfer H, Soveri P, Jarvilehto T.** Short-term habituation of the auditory evoked response in man. *Electroencephalogr Clin Neurophysiol* 28: 153–161, 1970.
- Gardner-Medwin AR, Tepley N, Barkley GL, Moran J, Nagel-Leiby S, Simkins RT, Welch KM.** Magnetic fields associated with spreading depression in anaesthetised rabbits. *Brain Res* 540: 153–158, 1991.
- Garrido MI, Friston KJ, Kiebel SJ, Stephan KE, Baldeweg T, Kilner JM.** The functional anatomy of the MMN: a DCM study of the roving paradigm. *Neuroimage* 42: 936–944, 2008.
- Garrido MI, Sahani M, Dolan RJ.** Outlier responses reflect sensitivity to statistical structure in the human brain. *PLOS Comput Biol* 9: e1002999, 2013.
- Gutfreund Y.** Stimulus-specific adaptation, habituation, and change detection in the gaze control system. *Biol Cybern* 106: 657–668, 2012.
- Haenschel C, Vernon DJ, Dwivedi P, Gruzeliér JH, Baldeweg T.** Event-related brain potential correlates of human auditory sensory memory-trace formation. *J Neurosci* 25: 10494–10501, 2005.
- Javitt DC, Steinschneider M, Schroeder CE, Vaughan HG, Jr., Arezzo JC.** Detection of stimulus deviance within primate primary auditory cortex: intracortical mechanisms of mismatch negativity (MMN) generation. *Brain Res* 667: 192–200, 1994.
- Koelsch S, Heinke W, Sammler D, Olthoff D.** Auditory processing during deep propofol sedation and recovery from unconsciousness. *Clin Neurophysiol* 117: 1746–1759, 2006.
- Kraus N, McGee T, Carrell T, King C, Littman T, Nicol T.** Discrimination of speech-like contrasts in the auditory thalamus and cortex. *J Acoust Soc Am* 96: 2758–2768, 1994.
- Kretzschmar B, Gutschalk A.** A sustained deviance response evoked by the auditory oddball paradigm. *Clin Neurophysiol* 121: 524–532, 2010.
- Lagarias J, Reeds JA, Wright H, Wright P.** Convergence properties of the Nelder-Mead simplex method in low dimensions. *SIAM J Optim* 9: 112–147, 1994.
- Lazar R, Metherate R.** Spectral interactions, but no mismatch negativity, in auditory cortex of anesthetized rat. *Hear Res* 181: 51–56, 2003.
- Lieder F, Daunizeau J, Garrido MI, Friston KJ, Stephan KE.** Modelling trial-by-trial changes in the mismatch negativity. *PLOS Comput Biol* 9: e1002911, 2013.
- May PJ, Tiitinen H.** Mismatch negativity (MMN), the deviance-elicited auditory deflection, explained. *Psychophysiology* 47: 66–122, 2010.
- Miyamoto M, Kawai J, Adachi Y, Haruta Y, Komamura K, Uehara G.** Development of an MCG/MEG system for small animals and its noise reduction methods. *J Phys* 97: 012258, 2008.
- Näätänen R, Gaillard AW, Mäntysalo S.** Early selective-attention effect on evoked potential reinterpreted. *Acta Psychol (Amst)* 42: 313–329, 1978.
- Näätänen R, Jacobsen T, Winkler I.** Memory-based or afferent processes in mismatch negativity (MMN): a review of the evidence. *Psychophysiology* 42: 25–32, 2005.
- Näätänen R, Kujala T, Escera C, Baldeweg T, Kreegipuu K, Carlson S, Ponton C.** The mismatch negativity (MMN)—a unique window to disturbed central auditory processing in ageing and different clinical conditions. *Clin Neurophysiol* 123: 424–458, 2012.
- Näätänen R, Paavilainen P, Alho K, Reinikainen K, Sams M.** Do event-related potentials reveal the mechanism of the auditory sensory memory in the human brain? *Neurosci Lett* 98: 217–221, 1989.
- Näätänen R, Paavilainen P, Rinne T, Alho K.** The mismatch negativity (MMN) in basic research of central auditory processing: a review. *Clin Neurophysiol* 118: 2544–2590, 2007.
- Nakamura T, Michie PT, Fulham WR, Todd J, Budd TW, Schall U, Hunter M, Hodgson DM.** Epidural auditory event-related potentials in the rat to frequency and duration deviants: evidence of mismatch negativity? *Front Psychol* 2: 367, 2011.
- Nelken I, Ulanovsky N.** Mismatch negativity and stimulus-specific adaptation in animal models. *J Psychophysiol* 21: 214–223, 2007.
- Nowak H, Giessler F, Huonker R, Hauelsen J, Röther J, Eiselt M.** A 16-channel SQUID device for biomagnetic investigations of small objects. *Med Eng Phys* 21: 563–568, 1999.
- Nuttall WJ, Clarke RH, Glowacki BA.** Resources: stop squandering helium. *Nature* 485: 573–575, 2012.
- Okada YC, Lähteenmki A, Xu C.** Experimental analysis of distortion of magnetoencephalography signals by the skull. *Clin Neurophysiol* 110: 230–238, 1999.
- Okada YC, Wu J, Kyuhou S.** Genesis of MEG signals in a mammalian CNS structures. *Electroencephalogr Clin Neurophysiol* 103: 474–485, 1997.
- Papanicolaou AC, Baumann S, Rogers RL, Saydjari C, Amparo EG, Eisenberg HM.** Localization of auditory response sources using magnetoencephalography and magnetic resonance imaging. *Arch Neurol* 47: 33–37, 1990.
- Pekkonen E, Hirvonen J, Jääskeläinen IP, Kaakkola S, Huttunen J.** Auditory sensory memory and the cholinergic system: implications for Alzheimer’s disease. *Neuroimage* 14: 376–382, 2001.
- Ritter W, Vaughan HG, Costa LD.** Orienting and habituation to auditory stimuli: a study of short term changes in average evoked responses. *Electroencephalogr Clin Neurophysiol* 25: 550–556, 1968.
- Roberts TP, Ferrari P, Stufflebeam SM, Pöppel D.** Latency of the auditory evoked neuromagnetic field components: stimulus dependence and insights toward perception. *J Clin Neurophysiol* 17: 114–129, 2000.
- Roberts TP, Pöppel D.** Latency of auditory evoked M100 as a function of tone frequency. *Neuroreport* 7: 1138–1140, 1996.
- Rogers RL, Papanicolaou AC, Baumann SB, Saydjari C, Eisenberg HM.** Neuromagnetic evidence of a dynamic excitation pattern generating the N100 auditory response. *Electroencephalogr Clin Neurophysiol* 77: 237–240, 1990.
- Rosburg T, Zimmerer K, Huonker R.** Short-term habituation of auditory evoked potential and neuromagnetic field components in dependence of the interstimulus interval. *Exp Brain Res* 205: 559–570, 2010.

- Salminen NH, May PJ, Alku P, Tiitinen H.** A population rate code of auditory space in the human cortex. *PLOS ONE* 4: e7600, 2009.
- Sambeth A, Maes JH, Van Luijtelaar G, Molenkamp IB, Jongma ML, Van Rijn CM.** Auditory event-related potentials in humans and rats: effects of task manipulation. *Psychophysiology* 40: 60–68, 2003.
- Särelä J, Valpola H.** Denoising source separation. *J Mach Learn Res* 6: 233–272, 2005.
- Siegel SJ, Connolly P, Liang Y, Lenox RH, Gur RE, Bilker WB, Kanes SJ, Turetsky BI.** Effects of strain, novelty, and NMDA blockade on auditory-evoked potentials in mice. *Neuropsychopharmacology* 28: 675–682, 2003.
- Simpson TP, Manara AR, Kane NM, Barton RL, Rowlands CA, Butler SR.** Effect of propofol anaesthesia on the event-related potential mismatch negativity and the auditory-evoked potential N1. *Br J Anaesth* 89: 382–388, 2002.
- Soros P, Teismann IK, Manemann E, Lutkenhoner B.** Auditory temporal processing in healthy aging: a magnetoencephalographic study. *BMC Neurosci* 10: 34, 2009.
- Taaseh N, Yaron A, Nelken I.** Stimulus-specific adaptation and deviance detection in the rat auditory cortex. *PLOS ONE* 6: e23369, 2011.
- Ulanovsky N, Las L, Farkas D, Nelken I.** Multiple time scales of adaptation in auditory cortex neurons. *J Neurosci* 24: 10440–10453, 2004.
- Ulanovsky N, Las L, Nelken I.** Processing of low-probability sounds by cortical neurons. *Nat Neurosci* 6: 391–398, 2003.
- Umbricht D, Vysotky D, Latanov A, Nitsch A, Brambilla R, D'Adamo P, Lipp HP.** Midlatency auditory event-related potentials in mice: comparison to midlatency auditory ERPs in humans. *Brain Res* 1019: 189–200, 2004.
- Umbricht D, Vysotky D, Latanov A, Nitsch R, Lipp HP.** Deviance-related electrophysiological activity in mice: is there mismatch negativity in mice? *Clin Neurophysiol* 116: 353–363, 2005.
- von der Behrens W, Buerle P, Kössl M, Gaese BH.** Correlating stimulus-specific adaptation of cortical neurons and local field potentials in the awake rat. *J Neurosci* 29: 13837–13849, 2009.
- Winkler I, Tervaniemi M, Näätänen R.** Two separate codes for missing-fundamental pitch in the human auditory cortex. *J Acoust Soc Am* 102: 1072–1082, 1997.
- Woods DL, Elmasian R.** The habituation of event-related potentials to speech sounds and tones. *Electroencephalogr Clin Neurophysiol* 65: 447–459, 1986.
- Yaron A, Hershenhoren I, Nelken I.** Sensitivity to complex statistical regularities in rat auditory cortex. *Neuron* 76: 603–615, 2012.
- Zhu Z, Zurner JM, Lowenthal ME, Padberg J, Recanzone GH, Krubitzer LA, Nagarajan SS, Disbrow EA.** The relationship between magnetic and electrophysiological responses to complex tactile stimuli. *BMC Neurosci* 10: 4, 2009.
- Zurner JM, Nagarajan SS, Krubitzer LA, Zhu Z, Turner RS, Disbrow EA.** MEG in the macaque monkey and human: distinguishing cortical fields in space and time. *Brain Res* 1345: 110–124, 2010.

